

## Responses to Reviewer #2

Dear Reviewer,

We sincerely thank you for your further constructive comments and suggestions on our work in the second round review; your comments substantially improved this paper. Our responses follow the “>>” signs in the response file and are marked in the revised manuscript with the “track changes” mode in word.

***1. Major Comments: In the last paragraph of section 3.3, the authors think the bad performance of the model in the last several years is due to the 2008 Olympic Games. However, the Olympic Games were in summer. There is no evidence showing that emissions in winter were affected. From the emission trends in responses to reviewers, SO<sub>2</sub>, dust and soot emissions do not have significant change from 2007 to 2009 in Beijing. In addition, the emissions have substantial decrease from 1995 to 2003, but the model predictions look fine. Therefore, it's questionable to attribute the phenomena to strict emissions control in 2008. The model explained fluctuations of hazy days from 1981 to 2015 without considering emission changes. During the last three decades, large changes in emissions occurred in China. This issue should be addressed before being published in ACP.***

>>Answer: We agree that the fluctuations of winter visibility and haze days since 1980s were inevitably influenced or modulated by the emission changes in BTH or even the larger areas. However, it's difficult to distinguish quantitatively the components caused by the emission changes due to the lack of the substantial or real emission data for each winter in these regions. We want to emphasize that the statistic models, theoretically, were designed to capture or reflect the fluctuations of the winter mean visibility (haze days) caused by the natural factors such as atmospheric circulations, especially on inter-annual time scales. Because the emission changes caused by the political actions were not predictable for the statistical model. Generally, the residual errors between the observed visibility (haze days) and the predicted could be attributed to the two aspects, namely the natural variability of atmospheric circulation and the changes of pollutant emissions. As for the forecast skill of the model decreased relatively in the last few years, it could be roughly attributed to the two aspects, although the contribution rates of each factor are not clear in this work. In the last paragraph of section 3.3 in the revised manuscript, we try to soften the speculation of the attribution analysis. We mentioned that the relative larger errors may be partly caused by the pollutant emissions changes. At present, it's not clear about the contribution rates of the natural variability

and the changes of pollutant emissions. Thus we call for more studies to better understand this issue.

## 2. Minor corrections:

**(1) It is kind of weird to use the phrase “hazy pollution”, recommend using “haze pollution”**

>>Answer: Well, the phrase “hazy pollution” have been changed to “haze pollution” in the revised manuscript.

**(2) Line 71, rewrite the sentence “dominant meteorological factors during heavy pollution in the BTH region”**

>>Answer: The sentence has been rewritten in the revised manuscript according to the suggestion.

**(3) Line 456, should be “significant” not “significantly”**

>>Answer: We corrected it in the revised manuscript.

**(4) In figure 9, it is hard to read whether the value is positive or negative. The author can use different colors to denote, like in figure 3.**

>>Answer: For consistency, both Figure 7, 8, 9 and 10 have been re-plotted. In the new figures, the positive values were presented by red lines and the negative values were presented by blue dashed lines with the exception of Figure 7 (vectors). The new figures are as follows:

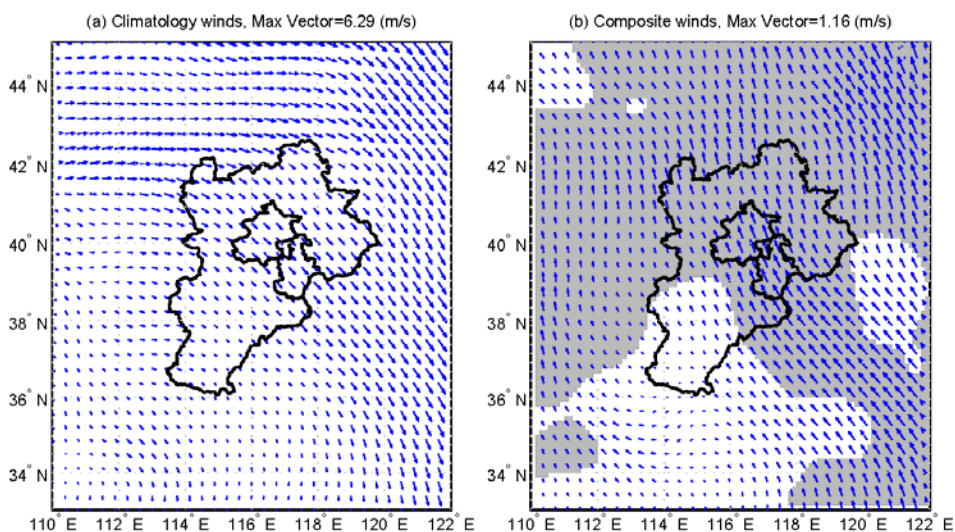


Figure 7 The climatological mean (a) and the composite (b) wind fields averaged from 1000 to 900 hPa (Area significant at the 0.05 level are shaded)

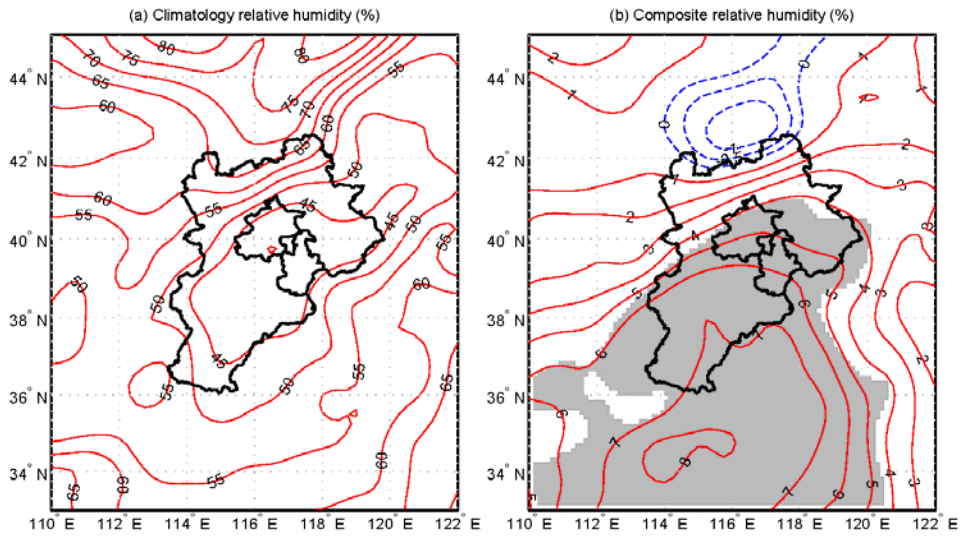


Figure 8 Same as Figure 7, but for relative humidity

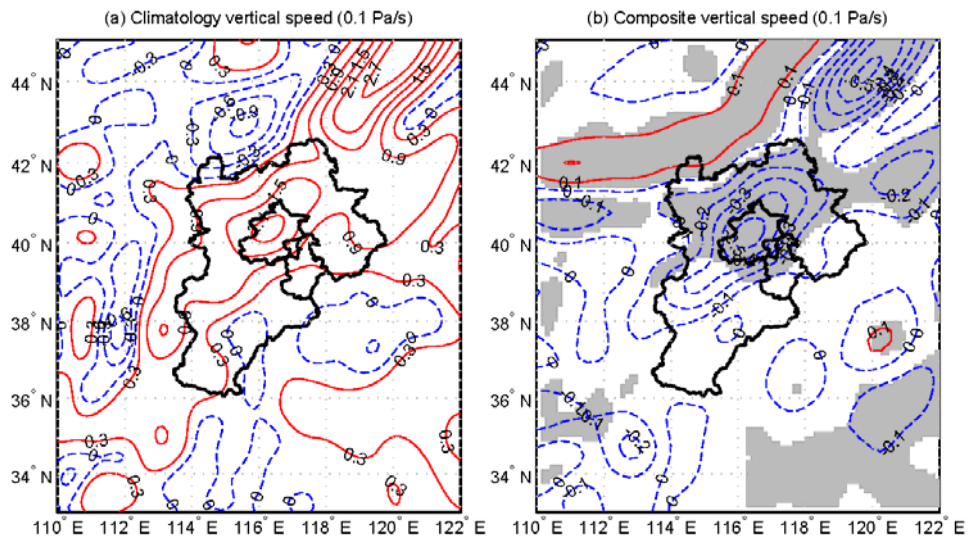


Figure 9 Same as Figure 7, but for vertical speed

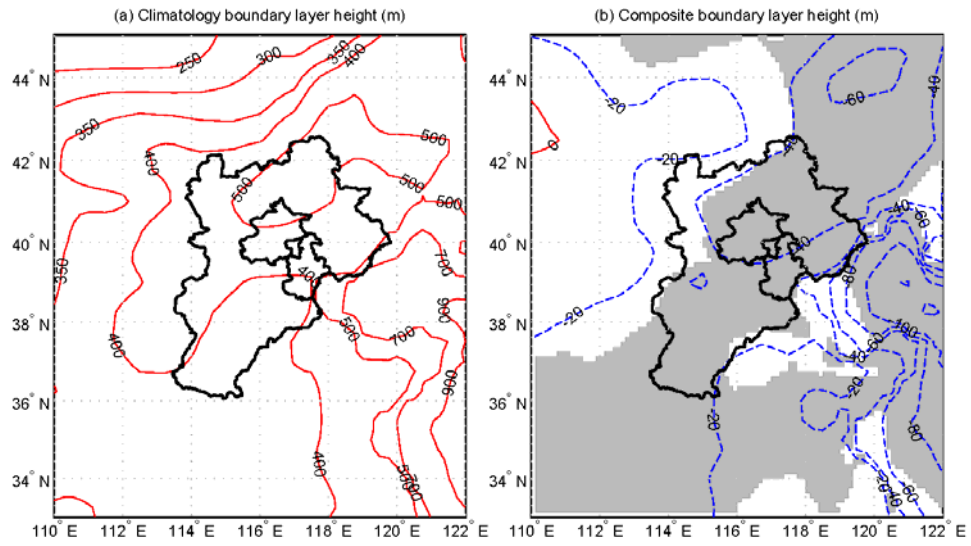


Figure 10 The climatological mean (a) and the composite (b) boundary layer height  
(Area significant at the 0.05 level are shaded)

1 Possible influence of atmospheric circulations on winter ~~hazy~~  
2 ~~pollution~~haze pollution in Beijing-Tianjin-Hebei region,  
3 northern China

4  
5 Ziyin Zhang<sup>1\*</sup>, Xiaoling Zhang<sup>1</sup>, Daoyi Gong<sup>2</sup>, Seong-Joong Kim<sup>3</sup>, Rui Mao<sup>2</sup>,  
6 Xiujuan Zhao<sup>1</sup>

7 <sup>1</sup>*Environmental Meteorology Forecast Center of Beijing-Tianjin-Hebei, Chinese*  
8 *Meteorological Administration, Beijing 100089, China*

9 <sup>2</sup>*State Key Laboratory of Earth Surface Processes and Resource Ecology, Beijing*  
10 *Normal University, Beijing 100875, China*

11 <sup>3</sup>*Korea Polar Research Institute, Incheon 406-840, Korea*  
12

13 **Abstract:**

14 Using the daily records derived from the synoptic weather stations and the  
15 NCEP/NCAR and ERA-Interim reanalysis data, the variability of the winter ~~hazy~~  
16 ~~pollution~~haze pollution (indicated by the mean visibility and number of hazy days) in  
17 Beijing-Tianjin-Hebei (BTH) region during the period 1981 to 2015 and its relationship  
18 to the atmospheric circulations in middle-high latitude were analyzed in this study. The  
19 winter ~~hazy~~haze pollution in BTH had distinct inter-annual and inter-decadal  
20 variabilities without a significant long-term trend. According to the spatial distribution  
21 of correlation coefficients, six atmospheric circulation indices ( $I_1$  to  $I_6$ ) were defined  
22 from the key areas in sea level pressure (SLP), zonal and meridional winds at 850 hPa  
23 (U850, V850), geopotential height field at 500 hPa (H500), zonal wind at 200 hPa  
24 (U200), and air temperature at 200 hPa (T200), respectively. All of the six indices have  
25 significant and stable correlations with the winter visibility and number of hazy days in  
26 BTH. In the raw (unfiltered) correlations, the correlation coefficients between the six  
27 indices and the winter visibility (number of hazy days) varied from 0.57 (0.47) to 0.76  
28 (0.6) with an average of 0.65 (0.54); in the high-frequency (<10 yr) correlations, the  
29 coefficients varied from 0.62 (0.58) to 0.8 (0.69) with an average of 0.69 (0.64). The  
30 six circulation indices together can explain 77.7% (78.7%) and 61.7% (69.1%)  
31 variances of the winter visibility and number of hazy days in the year-to-year (inter-

---

\* Correspondence to: Ziyin Zhang, Environmental Meteorology Forecast Center of Beijing-Tianjin-Hebei, Chinese Meteorological Administration, Beijing 100089, China.  
E-mail: zzy\_ahgeo@163.com

32 annual) variability, respectively. The increase of  $I_c$  (a comprehensive index derived  
33 from the six individual circulation indices) can cause a shallowing of the East Asian  
34 trough at the middle troposphere and a weakening of the Siberian high pressure field at  
35 sea level, and then accompanied by a reduction (increase) of horizontal advection and  
36 vertical convection (relative humidity) in the lowest troposphere and a reduced  
37 boundary layer height in BTH and its neighboring areas, which are favorable for the  
38 formation of ~~hazy pollution~~haze pollution in BTH winter, and vice versa. The high  
39 level of the prediction statistics and the reasonable mechanism suggested that the winter  
40 ~~hazy pollution~~haze pollution in BTH can be forecasted or estimated credibly based on  
41 the optimized atmospheric circulation indices. ~~However, we also noted that the statistic~~  
42 ~~estimation models would be largely influenced by the artificial control of a pollutant~~  
43 ~~discharge.~~ Thus it is helpful for government decision-making departments to take  
44 actions in advance in dealing with probably severe ~~hazy pollution~~haze pollution in  
45 BTH indicated by the atmospheric circulation conditions.

46 **Key word:** ~~hazy pollution~~haze pollution, visibility, atmospheric circulation, Beijing-  
47 Tianjin-Hebei,  
48

## 49 1 Introduction

50 Beijing-Tianjin-Hebei (BTH) region is located in northern China, with approximately  
51 110 million residents and 216,000 km<sup>2</sup> in size. As the rapid progress of urbanization  
52 and industrial development over the past three decades, the BTH region has become  
53 one of China's most economically developed regions and the third economic engine in  
54 China. Recently, the Chinese government has been promoting the integration of the  
55 three neighboring regions to optimize the industrial layout and improve the allocation  
56 of resources. Undoubtedly, the BTH region is becoming more and more important in  
57 China or even the world economy in the future. However, the rapid economic growth  
58 and urbanization have increased the level of air pollution in recent decades (Streets et  
59 al., 2007; Chan and Yao, 2008; Wang et al., 2009; Wang et al., 2010; Gao et al., 2011).  
60 Most of eastern China has frequently suffered from severe haze or smog days in recent  
61 years, especially in the BTH region. For example, the continuously ~~hazy pollution~~haze  
62 ~~pollution~~ in January 2013 greatly threatened human health and traffic safety (Kang et  
63 al., 2013; Wang et al., 2013). Roughly speaking, the ~~hazy pollution~~haze pollution can  
64 be attributed to two aspects: pollutant emissions to the lower atmosphere from fossil  
65 fuel combustion or construction and favorable meteorological conditions.

66 Meteorological conditions are controlling the occurrence of ~~hazy-pollution~~haze  
67 pollution (Wu, 2012; Zhang et al., 2013). Specifically, weather conditions play an  
68 essential role in the daily fluctuation of air pollutant concentrations (Zhang et al., 2015).

69 At present, many studies have focused on the physical and chemical properties of  
70 pollutants in Beijing and other cities (Feng et al., 2006; Yu et al., 2011; Xu et al., 2013;  
71 Zhao et al., 2013). And also studies demonstrated the influence of weather conditions  
72 or synoptic situations upon air pollutions (Zhao et al., 2009; Zhang et al., 2015). They  
73 elucidated clearly the formation and chemical composition of air pollutants and the  
74 dominant meteorological factors ~~on hazy days or~~ during heavy pollution in the BTH  
75 region-Beijing and its neighboring areas. On the other hand, some studies demonstrated  
76 that the ~~hazy-pollution~~haze pollution occurring in the BTH region could be strongly  
77 affected by the local atmospheric circulations including sea-land and mountain-valley  
78 breeze circulations and the planetary boundary layer height (Lo et al., 2006; Liu et al.,  
79 2009; Chen et al., 2009; Miao et al., 2015). Recently, Wang et al. (2015) suggested that  
80 the reduction of autumn Arctic sea ice leads to anomalous atmospheric circulation  
81 changes which favor less cyclone activity and more stable atmosphere and leading to  
82 more hazy days in eastern China. Moreover, Wang et al. (2013) showed that east China  
83 suffered from severe ~~hazy-pollution~~haze pollutions in January 2013 may be due to a  
84 sudden stratospheric warming over the mid-high latitude of Northern Hemisphere,  
85 which lead to an anomalous steady atmosphere dominated in northern China. Thus, it  
86 is interesting to examine whether the winter ~~hazy-pollution~~haze pollution in BTH has  
87 been influenced by other known or unknown atmospheric circulations or  
88 teleconnections in the mid-high latitude of the Northern Hemisphere and whether there  
89 are some potential circulations that can be used for the forecast or evaluation of the  
90 winter ~~hazy-pollution~~haze pollution in BTH. To date, it is not clear about these  
91 questions, and a few studies have been performed to explore these issues.

92 Owing to a lack of long-term instrumental records for air pollutant concentration,  
93 the understanding of the evolution of air pollution and their relations to atmospheric  
94 circulations is limited. In this paper, we intend to use the atmospheric visibility and the  
95 number of hazy days derived from the synoptic meteorological stations to denote the  
96 evolution of ~~hazy-pollution~~haze pollution in the BTH region since 1980s. Many studies  
97 demonstrated that, in the absence of certain weather conditions (e.g., rain, fog, dust and  
98 snowstorm), the visibility is an excellent indicator of air quality because its degradation  
99 results from light scattering and absorption by atmospheric particles and gases that can  
100 originate from natural or anthropogenic sources (Baumer et al., 2008; Chang et al., 2009;

101 Sabetghadam et al., 2012; Baddock et al., 2014), although visibility was influenced  
102 comprehensively by airborne pollutants and meteorological parameters such as relative  
103 humidity, wind speed, temperature, pressure and solar radiation (Wen and Yeh, 2010;  
104 Deng et al., 2014; Zhang et al., 2015) .

105 The main purpose of this study is to examine the possible relations between the  
106 atmospheric circulations and the winter ~~hazy pollution~~haze pollution (the mean  
107 visibility and mean number of hazy days) over the BTH region and investigate the  
108 possible physical mechanism, which could be useful for a prediction of the winter ~~hazy~~  
109 ~~pollution~~haze pollution and could provide a scientific support to the government to take  
110 effective measures in advance to reduce or control the pollutant emission in case of an  
111 anomalous circulations leading to a serious ~~hazy pollution~~haze pollution in the region.  
112 This paper is organized as follows. Section 2 describes the data and method used.  
113 Section 3 shows major results and discussions. Conclusion is summarized in section 4.

## 114 2 Data and methods

### 115 2.1 Research area and station data

116 The atmospheric visibility recorded at the 19 synoptic meteorological stations  
117 located in the research area from 1 January 1980 to 28 February 2015 were used (Figure  
118 1). The visibility by human observers is recorded by four times (02:00, 08:00, 14:00  
119 and 20:00, Beijing local time) or three times (08:00, 14:00 and 20:00, Beijing local time)  
120 per day. A good continuous monitoring operation was maintained throughout the entire  
121 period, with the missing data rates for the 19 stations varying from a minimum of 1.7%  
122 to a maximum of 2.1%, with a mean 1.9%. On the other hand, the distribution of the  
123 stations is relatively uniform, indicating that the mean visibility or hazy days is a good  
124 representative for the whole BTH region.

125 In the present study, the days with visibility  $\leq 5$  km and relative humidity  $< 90\%$   
126 at 14:00PM (local time) were defined as hazy days, except the special weather  
127 phenomena occurred at this moment including rain, fog, dust and snow (Schichtel et al.,  
128 2010; Wu et al., 2014; ). The mean number of hazy days ( $\overline{NHD}$ ) of each winter in the  
129 BTH region can be calculated by:

$$130 \quad \overline{NHD} = \frac{1}{n} \sum_{i=1}^n N_i \quad (1)$$

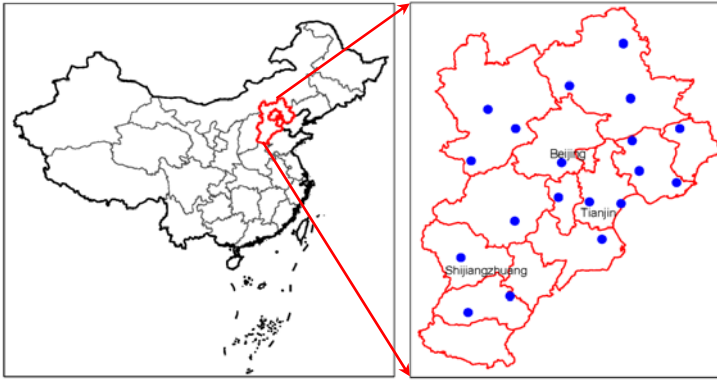
131 where  $n$  is the number of stations (here  $n=19$ ),  $N$  denotes the number of hazy days  
132 in a station in each winter (December, January and February). The mean visibility ( $\overline{Vis}$ )



133 of each winter in the BTH region can be calculated by:

134 
$$\overline{Vis} = \frac{1}{n} \sum_{i=1}^n \left( \frac{1}{m} \sum_{j=1}^m V_{ij} \right) \quad (2)$$

135 where  $n$  is the number of stations (here  $n=19$ ),  $m$  is the number of valid days in  
136 winter. It should be noted that the winter in 1981 consists of December 1980, January  
137 and February 1981, and so on.



138  
139 Figure 1 Research area and locations of the 19 synoptic meteorological stations

## 140 2.2 Reanalysis data

141 The global NCEP/NCAR reanalysis data of the monthly sea level pressure (SLP),  
142 zonal and meridional winds at 850 hPa (U850, V850), geopotential height field at 500  
143 hPa (H500), zonal wind at 200 hPa (U200) and air temperature at 200, 150, 100 and 70  
144 hPa (T200, T150, T100, T70) with a  $2.5^\circ \times 2.5^\circ$  spatial resolution from January 1980 to  
145 February 2015 were used (Kalnay et al., 1996). Moreover, in order to obtain a higher  
146 spatial resolution in the BTH region, the ERA-Interim reanalysis data of the monthly  
147 relative humidity (RH), vertical speed (W), zonal (U) and meridional (V) winds from  
148 1000 to 500 hPa (16 pressure levels in total) and the boundary layer height (BLH) with  
149 a  $0.125^\circ \times 0.125^\circ$  spatial resolution confined to the area  $33\text{-}45^\circ\text{N}$  and  $110\text{-}122^\circ\text{E}$  were  
150 also used (Dee et al., 2011).

## 151 2.3 Analysis method

152 For the statistical and atmospheric circulation analyses carried out in the study, the  
153 common statistical methods such as the composite analyses and the least square  
154 regression and the Pearson correlation analyses with a two-tailed Student's t-test were  
155 applied in this research. A principal component analysis (PCA) was also used to extract  
156 the principal mode of multiple time series. Moreover, in order to reduce the possible  
157

158 effects of low-frequency variation or long-term trends and to examine whether or not  
159 the correspondence between the two time series on inter-annual time-scale is stable, the  
160 high-frequency (< 10yr) correlation of the high-pass filtered time series was also tested  
161 for time series analyses (Gong and Luterbacher, 2008; Zhang et al., 2010).

162

### 163 **3 Results and discussions**

#### 164 **3.1 Evolution of the winter visibility and hazy days in the BTH region**

165 The regional mean visibility and number of hazy days in winter in BTH were  
166 presented in Figure 2. As expected, the visibility was negatively correlated to the  
167 number of hazy days with the raw and high-frequency (< 10yr) correlation coefficients  
168 between them of -0.91 and -0.93, respectively. Both of them are significant at the 0.01  
169 level ( $p < 0.01$  for short). More hazy days generally denote lower mean visibility in  
170 winter due to the light scattering and absorption effects of air pollutants (Baumer et al.,  
171 2008; Sabetghadam et al., 2012). There are intense inter-annual fluctuations in both the  
172 visibility and the number of hazy days over the entire period of 1981 to 2015. The  
173 decadal fluctuations can be also distinguished for both the visibility and the number of  
174 hazy days throughout the entire period. A significant reducing trend of visibility  
175 ( $p < 0.05$ ) and increasing trend of number of hazy days ( $p < 0.01$ ) dominated in the 1980s.  
176 And then, the visibility experienced an increasing trend in 1990s and a decreasing trend  
177 since 2001, and the hazy days showed an anti-phase changes, but none of them are  
178 statistically significant with exception of the number of hazy days trend in 1990s  
179 ( $p < 0.05$ ). The mean visibility maximum in 1990s reached to 18.3 km (larger than the  
180 mean values of 17.9 km over the entire period); and the minimum number of hazy days  
181 in 1990s reached to 20.6 days (less than the mean values of 22.7 days over the entire  
182 period). However, the long-term trends of them are not statistically significant, although  
183 a weak reducing and increasing trends can be founded in the curves of winter visibility  
184 and number of hazy days, respectively.

185

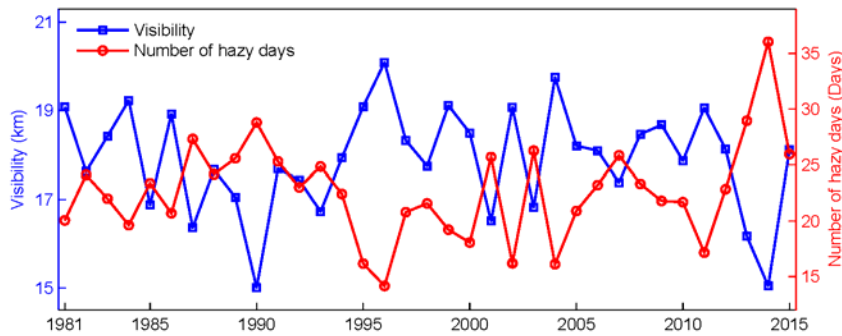


Figure 2 Curves of the winter mean visibility and number of hazy days in BTH

### 3.2 Relationship between ~~hazy pollution~~haze pollution and atmospheric circulations

We first examined the correlation coefficients between the visibility and number of hazy days and the most common atmospheric teleconnection or oscillation indices over the mid-high latitude of Northern hemisphere (see Table 1), which could affect the winter climate variability over China, such as the Arctic Oscillation (AO), the Northern Atlantic Oscillation (NAO), the Pacific/North American pattern (PNA), the Eurasian pattern (EU), the Western Pacific pattern (WP) and the Siberian High (SBH) (Wallace and Gutzler, 1981; Zhang et al., 2009; Gong and Ho, 2012). It can be seen that both of the raw ( $r_1$ ) and high-frequency ( $r_2$ ) correlations show that the visibility and number of hazy days are correlated weakly with the winter AO, NAO and PNA. However, the visibility is highly positively correlated with EU, WP and SBH; and the number of hazy days is highly negatively correlated with EU, WP and SBH, most of them are significant at the 0.01 or 0.05 level.

Table 1 Correlation coefficients of visibility and hazy days and circulation indices

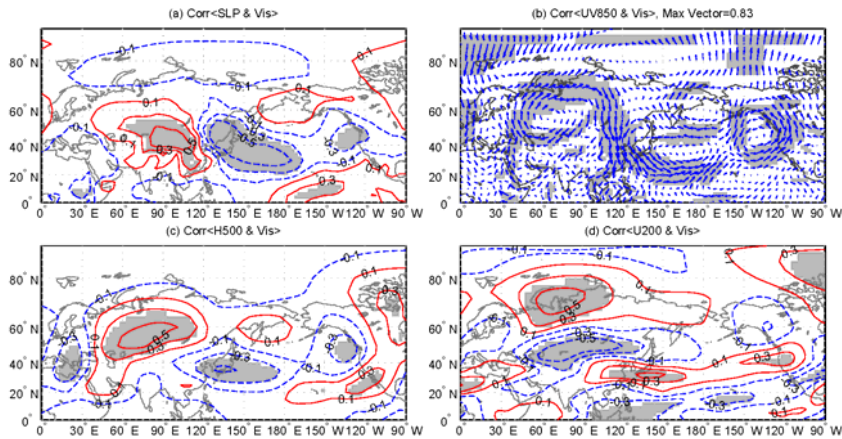
		AO	NAO	PNA	EU	WP	SBH
Visibility	$r_1$	-0.11	0.00	0.16	0.61**	0.40*	0.39*
	$r_2$	0.05	0.22	0.16	0.71**	0.37*	0.36*
Number of hazy days	$r_1$	0.13	0.13	-0.10	-0.51**	-0.47**	-0.32
	$r_2$	-0.01	-0.11	-0.10	-0.70**	-0.56**	-0.37*

\*\* Significant at the 0.01 level, \* Significant at the 0.05 level. The  $r_1$  and  $r_2$  terms indicate the raw correlation and high-frequency (< 10yr) correlation, respectively.

Furthermore, the general characteristics of spatial distribution of the correlation

208 coefficients between visibility and number of hazy days in BTH and the major  
209 meteorological fields from surface to tropopause in Northern Hemisphere including  
210 SLP, U850, V850, H500, U200, T200, T150 and T70 were also examined (Figure 3 and  
211 4). Owing to a generally anti-pattern for the number of hazy days, thus only the  
212 correlation maps with visibility were analyzed for simplicity. In SLP (Figure 3a), a  
213 positive correlation center dominated most of East Asian continent, while a negative  
214 correlation center dominated the area from northeast Asia to northwest Pacific,  
215 respectively. This spatial pattern may reflect the effects of land-sea thermal contrast on  
216 the lower troposphere condition over BTH region. The pressure increasing in East  
217 Asian continent and decreasing in area from northeast Asia to northwest Pacific suggest  
218 that they favor the visibility increase in the BTH region in winter, and vice versa. In  
219 UV850 (Figure 3b), an anomalously anti-cyclonic and northerly pattern are  
220 predominant most of Siberia and eastern China. This suggests that an anomalous  
221 northerly advection from Siberian to eastern China improve the winter visibility in the  
222 BTH region. In H500 (Figure 3c), there exist a “-+-” wave train pattern along the  
223 Eurasia-west Pacific in the mid-high latitude, extending from the central-eastern  
224 Europe through Siberia to north China-Korean peninsula-Japan-northwest Pacific  
225 Ocean, similar to the EU pattern (Wallace and Gutzler, 1981). This pattern implies that  
226 a deepening of East Asian trough and a weakening of blocking will favor the winter  
227 visibility increase in the BTH region. In U200 (Figure 3d), there also exist a wave train  
228 pattern from northwest Russia through Siberia to northwest Pacific Ocean. This pattern  
229 may imply that the south (north) of East Asian Jet stream strengthened (weakened)  
230 coincided with the anomalous ascending (sinking) motions occurred in the south (north)  
231 of the Jet stream entrance at the upper troposphere, which will lead to a strengthening  
232 northerly appeared in the lower troposphere. Hence it is not conducive to the  
233 accumulation of pollutants over BTH region in the winter.

234



235  
 236 Figure 3, Spatial distribution of correlation coefficients between visibility and SLP (a), UV850  
 237 (b), H500 (c) and U200 (d) (Area significant at the 0.05 level are shaded; either U850 or V850  
 238 significant at the 0.05 level are shaded in b)  
 239

240 Besides the lower troposphere, previous studies suggested that the anomalous  
 241 stratospheric warming over the Northern Hemisphere led to the severe ~~hazy~~  
 242 ~~pollution~~~~haze~~ ~~pollutions~~ in east China in January 2013 (Wang et al., 2013). Here, the  
 243 spatial distribution of the correlation coefficients between visibility and the temperature  
 244 from the upper troposphere to lower stratosphere at 200 hPa (T200), 150 hPa (T150),  
 245 100 hPa (T100) and 70 hPa (T70) were checked. Negative correlations are found from  
 246 eastern Siberia to the northern North Pacific including Alaska in T200, T150, T100 and  
 247 T70, respectively (Figure 4), with the biggest correlation in T200 (Figure 4a). The  
 248 significantly negative correlation suggest that the warming at 200 hPa over eastern  
 249 Siberia to the northern North Pacific would indicate a decreasing of winter visibility,  
 250 namely a worsening of ~~hazy~~~~pollution~~~~haze~~ ~~pollutions~~ in the BTH region.  
 251

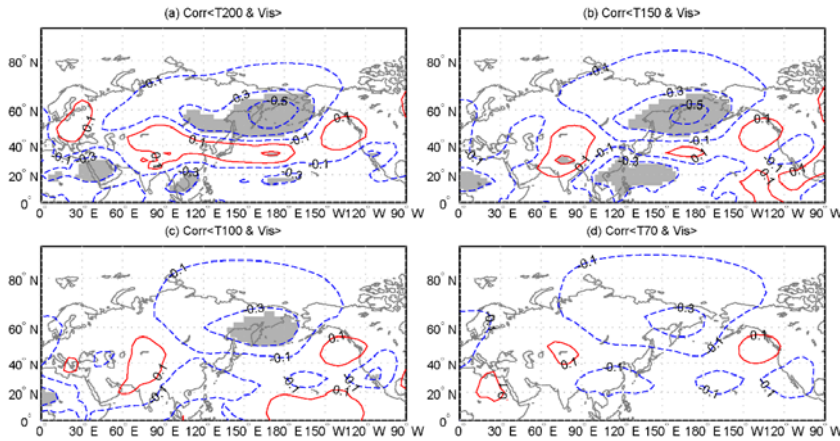


Figure 4 Spatial distribution of correlation coefficients between visibility and T200 (a), T150 (b), T100 (c) and T70 (d) (Area significant at the 0.05 level are shaded)

Based on the above analyses, we wonder whether the meteorological variables in the significant correlation areas can be used to predict or evaluate the variability of the winter visibility and ~~hazy pollution~~haze pollution in the BTH region. Thus, the six indices for atmospheric circulations or teleconnections were defined based on the key regions shown in the previous correlation maps as listed in Table 2. We computed the raw and high-frequency correlation coefficients of the winter visibility and number of hazy days in BTH and the six atmospheric circulation indices. All of the six indices ( $I_1$  to  $I_6$ ) show highly positive or negative correlations with the winter visibility and number of hazy days, with significance at the 0.01 level (Table3). Moreover, we note that most of the high-frequency correlations are larger than the raw correlations except the correlations between visibility and  $I_1$ . This suggests that the links between the air quality in BTH and the circulations indices are very stable from year to year. The significantly positive or negative correlations should be a reflection of the physical response mechanisms between them, which will be discussed in the latter section.

Table 2 List of the definition for the six circulation indices

Index	Variable	Expression
$I_1$	SLP	SLP (38~50N, 84~108E) – SLP (36~52N, 126~150E; 24~40N, 150~184E)
$I_2$	$U_{850hPa}$	$U_{850}$ (55~75N, 40~110E) – $U_{850}$ (40~50N, 45~75E)
$I_3$	$V_{850hPa}$	$V_{850}$ (32~64N, 104~120E)
$I_4$	$H_{500hPa}$	$H_{500}$ (46~64N, 50~92E) – $H_{500}$ (28~44N, 16~28E; 28~42N, 120~156E)

I <sub>5</sub>	U <sub>200hPa</sub>	U <sub>200</sub> (42~52N,60~110E) –U <sub>200</sub> (64~76N,50~96E; 28~36N, 120~152E)
I <sub>6</sub>	T <sub>200hPa</sub>	T <sub>200</sub> (46~66N, 146~196E)

272

273

274

Table 3 Correlation coefficients of visibility and number of hazy days and circulation indices

		I <sub>1</sub>	I <sub>2</sub>	I <sub>3</sub>	I <sub>4</sub>	I <sub>5</sub>	I <sub>6</sub>
Visibility	r1	0.73**	0.57**	-0.76**	0.62**	-0.59**	-0.61**
	r2	0.70**	0.68**	-0.80**	0.72**	-0.62**	-0.62**
Number of hazy days	r1	-0.60**	-0.47**	0.60**	-0.47**	0.52**	0.60**
	r2	-0.61**	-0.65**	0.69**	-0.67**	0.58**	0.64**

275

Same as Table 1

276

### 277 3.3 Predictions for visibility and number of hazy days based on the circulation 278 indices

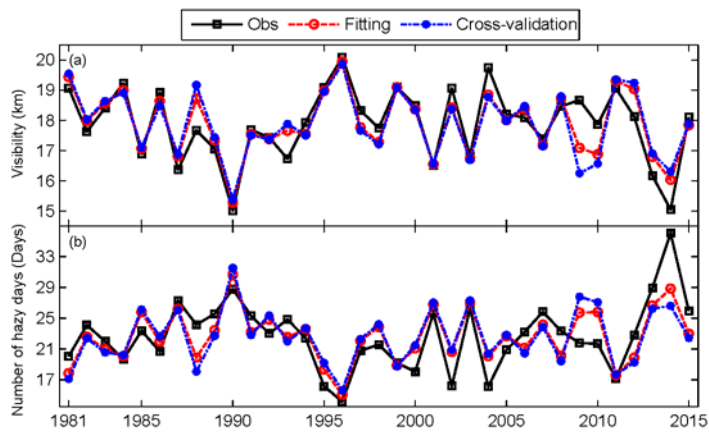
279 In order to assess the prediction capability of the six circulation indices for the  
280 winter ~~hazy pollution~~haze pollutions in BTH, the winter mean visibility and number of  
281 hazy days were estimated by applying a multivariate regression method with the least  
282 square estimate. The estimated curves by the fitting and the cross-validation with a  
283 leave-one-out method were displayed in Figure 5. Intuitively, both of the fitting curves  
284 and the cross-validation curves are fairly consistent with the observed winter mean  
285 visibility and number of hazy days over the last three decades. The raw and high-  
286 frequency correlation coefficients between the observed and the fitting visibility  
287 (number of hazy days) are 0.88 (0.78) and 0.86 (0.77), respectively. All of them are  
288 significantly at 0.01 level. The six circulation indices together can explain 77.7%  
289 (78.7%) and 61.7% (69.1%) variances of the winter visibility and number of hazy days  
290 over the BTH region in the year to year (inter-annual) variability, respectively. A good  
291 fitting does not mean that there must be stable relationships between the dependent  
292 variable and explanatory variables. Thus we emphasized testing the stability of the  
293 statistic models by means of the Leave-N-out cross-validations. The statistics for the  
294 cross-validation estimations were listed in Table 4, including the explained variance  
295 ( $r^2$ ), the standard error (SE), and reduction of error (RE). Previous studies suggested  
296 that RE is an extremely rigorous verification statistic because it has no lower bound,  
297  $RE > 0$  indicating the skillful estimation,  $RE > 0.2$  indicating the reliable estimation  
298 and  $RE = 1.0$  indicating a perfect estimation (Fritts, 1976; Gong and Luterbacher, 2008;  
299 Zhang et al., 2010).

300 The statistics for both the visibility and number of hazy days are generally stable  
301 (no sharply increase or decrease) when N increased from 1 to 11 (more than 30% sample  
302 removed in regression models), although the  $r^2$  and RE (SE) slightly decreased  
303 (increased) with the increasing of N. For the visibility, the  $r^2$  varied from 52.5% to 62.7%  
304 with an average of 57.6%, the SE varied from 0.74 to 0.84 with an average of 0.79, the  
305 RE varied from 0.49 to 0.61 with an average of 0.55. For the number of hazy days, the  
306  $r^2$  varied from 31.1% to 41.5% with an average of 35.2%, the SE varied from 3.37 to  
307 3.66 with an average of 3.54, the RE varied from 0.23 to 0.38 with an average of 0.30.  
308 The mildly changes of these statistics suggest that the statistic models between the given  
309 atmospheric circulations and the ~~hazy pollution~~haze pollution indicators are stably even  
310 in the case of parts of sample missed. On the other hand, we noted the statistics for the  
311 visibility estimations are generally better than that for the number of hazy days  
312 estimations in all tests. However, the minimum values of  $r^2$  and RE for the number of  
313 hazy days estimations are still lager than 30% and 0.2, respectively. Based on these  
314 statistics, it can be concluded that the predictions for the winter visibility and number  
315 of hazy days in the BTH region based on the circulation indices are overall reliable  
316 during the entire period, especially for the mean visibility. That is to say, the winter  
317 ~~hazy pollution~~haze pollutions in BTH can be evaluated or estimated well by the  
318 optimized atmospheric circulations.

319 The relatively larger errors for the estimated values referred to the observed  
320 visibility and number of hazy days have been found since the winter in 2009 (Figure 5).  
321 We re-computed all the statistics for the period 1981 to 2008, the results displayed that  
322 all the values of  $r^2$  and RE (SE) for visibility and number of hazy days predictions  
323 increased (decreased) much more than the entire period (Table 4), suggesting that the  
324 statistic estimation models are much more stable and reliable before 2009. Why did the  
325 prediction efficiency of the statistic estimation models decrease relatively in the last  
326 few years? It can be distinguished that the estimations for the winter mean visibility are  
327 distinctly lower (higher) than the observed in the winters of 2009 and 2010 (2014), and  
328 vice versa for the number of hazy days. We speculated that these phenomena can be  
329 attributed partly to the fluctuations of pollutant emissions ~~in part~~ because the pollutant  
330 emissions over northern China around 2008 were controlled strictly by the Chinese  
331 government associated with the 2008 Olympic Games in Beijing (An et al., 2007;  
332 Zhang et al., 2010; Gao et al., 2011). The decrease of pollutant emissions led to the  
333 improvement of air quality (increasing visibility and decreasing hazy days) in 2009 and  
334 2010, although the atmospheric conditions remained the same and did not contributed



335 to the spread and elimination of air pollutants. However, pollutant emissions especially  
 336 in the areas of BTH rebounded after the Olympic Games, with the decrease in visibility  
 337 and increase in hazy days in the BTH region around 2012 to 2014 to some extent (Zhang  
 338 et al., 2015), although the atmospheric conditions remained relatively the same as  
 339 before. From this result, it can be assumed the statistic estimation models for the winter  
 340 mean visibility and number of hazy days would be largely influenced by an artificial  
 341 control of pollutant discharge. Generally, the errors between the observed visibility (hazy days)  
 342 and the predicted could be attributed to the natural variability of atmospheric circulation and the  
 343 changes of pollutant emissions. However, the contribution rates of each factor are not clear now,  
 344 thus further studies will be necessary to unravel these issues.



346  
 347 Figure 5 Curves of the observed and the predicted winter visibility (a) and number of hazy days  
 348 (b) in the BTH region since 1981

349  
 350 Table 4 List of the statistics for the Leave-N-out cross-validation estimations

N	Period covering	Visibility			Number of hazy days		
		$r^2$ (%)	SE	RE	$r^2$ (%)	SE	RE
1	1981-2015	62.7	0.74	0.61	41.5	3.37	0.38
	1981-2008	87.1	0.42	0.87	53.9	2.56	0.52
3	1981-2015	56.8	0.80	0.54	34.3	3.57	0.28
	1981-2008	86.8	0.42	0.87	52.6	2.59	0.51
5	1981-2015	59.2	0.78	0.57	35.3	3.54	0.30
	1981-2008	86.8	0.42	0.87	46.7	2.75	0.43

7	1981-2015	59.0	0.78	0.56	37.5	3.48	0.33
	1981-2008	86.4	0.43	0.86	44.7	2.80	0.41
9	1981-2015	56.2	0.80	0.54	32.5	3.62	0.27
	1981-2008	84.2	0.46	0.84	40.8	2.90	0.36
11	1981-2015	52.5	0.84	0.49	31.1	3.66	0.23
	1981-2008	84.4	0.46	0.84	48.2	2.71	0.44

351 (N denotes the number of sample removed in the cross-validation regressions; only the odd  
352 numbers of N were listed for short)

353

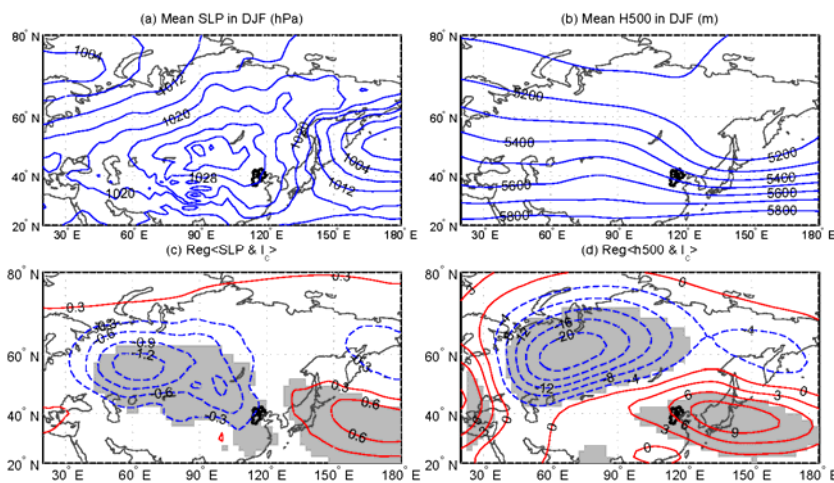
### 354 **3.4 Possible mechanism of the circulations related to the winter ~~hazy-~~** 355 **pollutionhaze pollutions**

356 In order to explore the possible mechanism and role of the investigated circulation  
357 indices on the winter visibility and number of hazy days in the BTH region, the links  
358 between the given large-scale atmospheric circulations and the local meteorological  
359 conditions, which have close relations with the ~~hazy-pollutionhaze~~ pollutions, were  
360 examined. For simplicity, a comprehensive index labeled as  $I_c$  was synthesized from  
361 the six individual circulation indices ( $I_1$  to  $I_6$ ) by applying a PCA method, namely the  
362 first principal component (PC1). The high values of the explained variance (64.4% in  
363 PC1) indicated that the comprehensive index of  $I_c$  roughly reflect the integrated features  
364 of all the six indices. Thus, we used the  $I_c$  instead of the six individual indices in the  
365 following analysis. Generally, the positive (negative)  $I_c$  indicate the lower (higher)  
366 visibility and more (less) hazy days in the BTH region in winter.

367 First we examined the links between the  $I_c$  and the meteorological fields of SLP  
368 and H500 respectively. Based on the NCEP/NCAR reanalysis data, Figure 6(a) and (b)  
369 present the climatological mean of SLP and H500 in winter averaged from 1981 to 2010,  
370 respectively. The changes of SLP and H500 in winter in association with a one-  
371 standard-deviation positive  $I_c$  during the winters 1981 to 2015 are shown in Figure 6(c)  
372 and (d), respectively. In the climatological mean fields, the BTH region were located in  
373 the trough of East Asian trough at the middle troposphere and in the ridge of Siberian-  
374 Mongolia high in SLP field, which indicate the northerly dominated the BTH region in  
375 winter. The regression maps show that the SLP decreased in the Siberian-Mongolia high  
376 areas and increased in the western Pacific in SLP and the geopotential height decreased  
377 in the most areas of Siberia and increased in the northern China to western Pacific.  
378 These patterns suggest that both the East Asian trough and Siberian high weaken with  
379 increasing  $I_c$ , that further implies that the winter cold air activity will be weaken and

380 then lead to an anomalous steady atmospheric conditions in BTH and its adjacent areas  
 381 in winter. Namely, the less strong Siberian high and East Asian trough and associated  
 382 northerly winds in the low and middle troposphere will lead to a severe **hazy**  
 383 **pollutionhaze pollution** (lower visibility and more hazy days) due to the favorable  
 384 meteorological conditions for the accumulation and chemical reaction of pollutants.  
 385 Anyway, we wonder whether it is true as we speculated. We further examined the links  
 386 between the comprehensive index of  $I_c$  and the local meteorological conditions which  
 387 play direct roles in the formation of **hazy pollutionhaze pollutions**, including the wind  
 388 fields (Figure 7), relative humidity (Figure 8) and vertical velocity (Figure 9) at the  
 389 lowest troposphere (averaged from 1000 hPa to 900 hPa with an interval of 25 hPa) and  
 390 the boundary layer height (Figure 10) based on the ERA-Interim reanalysis data.

391  
 392



393  
 394 Figure 6 The climatological mean fields of SLP (a) and H500 (b) averaged in winter 1981 to 2010,  
 395 and the spatial distribution of the regression coefficients of SLP (c) and H500 (d) upon the  $I_c$  over  
 396 the period 1981 to 2015 (Area significant at the 0.05 level are shaded)

397  
 398 Figure 7(a) displays the climatological mean wind field averaged from 1000 to 900  
 399 hPa over the winter 1981 to 2010. At lower level, the northwesterly winds dominated  
 400 the BTH, and the wind speed in Beijing, Tianjin and north of Hebei province was larger  
 401 than that in the south of Hebei province. Figure 7(b) shows the composite (positive  $I_c$   
 402 winters minus negative  $I_c$  winters) wind field averaged from 1000 to 900 hPa over the  
 403 winter 1981 to 2015. In the composite wind field, the anomalous southeasterly winds

404 dominated the BTH region instead of the northwesterly in the climatological mean wind  
405 field, indicating the weakening of the northwesterly significantly over BTH and its  
406 neighboring areas when  $I_c$  increased. Previous studies (Zhang et al., 2015) demonstrated  
407 the decreasing of wind speed is not conducive to the diffusion of air pollutants and  
408 easily lead to ~~hazy pollution~~haze pollutions in Beijing. It may be true for the whole  
409 BTH region. Thus, the increasing of  $I_c$  will lead to a decrease in the visibility and  
410 increase in the number of hazy days in winter over the BTH region.

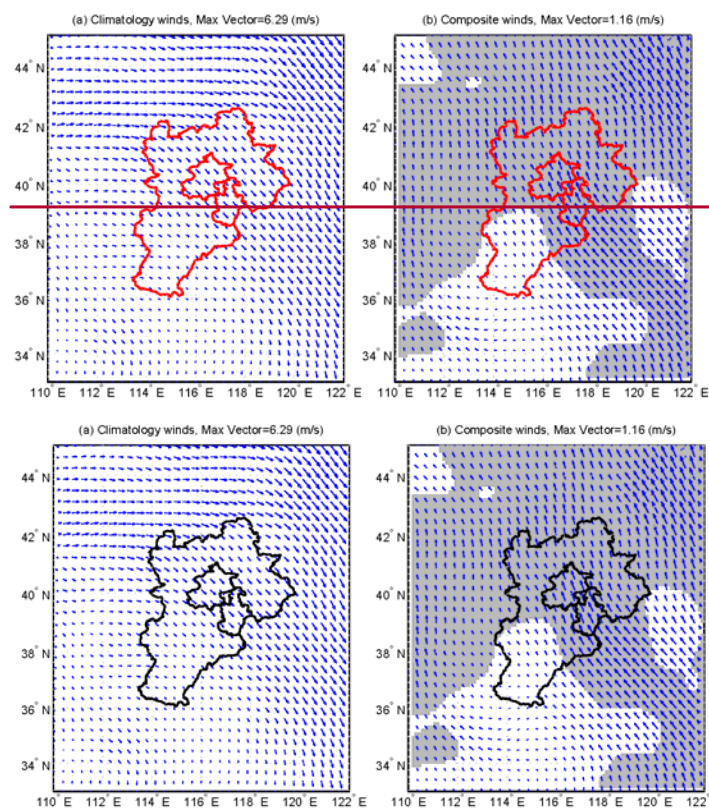
411 Same as Figure 7, Figure 8(a) and (b) present the climatology and composite  
412 relative humidity averaged from the lowest troposphere respectively. In the composite  
413 map, all the areas of BTH are covered by the positive values and most of them are  
414 significant at the 0.05 level. They indicate that the winter relative humidity was  
415 anomalous higher in the positive  $I_c$  years than that in the negative  $I_c$  years. As pointed  
416 in the Introduction, a high relative humidity is one of the important reasons for visibility  
417 degradation. This is because that the high relative humidity is favorable for the accumulation and  
418 hygroscopic growth of pollutants, which can strengthen the light scattering and absorption by  
419 atmospheric particles and gases and then cause the visibility degradation directly (Baumer et al.,  
420 2008; Zhang et al., 2015). Thus a positive  $I_c$  imply that a decreasing of visibility  
421 accompanied by the increasing number of hazy days may occur in the winter over BTH  
422 region. Figure 9(a) and (b) present the climatology and composite vertical speeds  
423 averaged from the lowest troposphere respectively. The positive (negative) values of  
424 vertical speed in unit of Pa/s denote sinking (ascending) motion. The climatological  
425 vertical speeds show that the downward air motions dominated the BTH region in the  
426 winter. In the composite vertical speed field, the most areas of BTH were covered by  
427 the significantly negative values, which suggested a less vertical exchanges of air  
428 occurred in this areas in the positive  $I_c$  winters. In other words, the increased  $I_c$  may  
429 result in a weaker vertical convection and forcing the lowest troposphere more stable.  
430 It's easy to understand the anomalous stabilization will lead to much ~~hazy pollution~~haze  
431 pollutions. Moreover, a similar result can be found in the planetary boundary layer  
432 height, which was reduced significantly in the most of BTH and its adjacent areas in  
433 the positive  $I_c$  winters (Figure 10). The decreased boundary layer height will depress  
434 the air pollutants into a narrower air column in a certain area and then lead to an  
435 increasing of the pollutants concentration. Thus, a winter with the lower visibility and  
436 more hazy days in the BTH region would be expected in the case of the lower boundary  
437 layer height caused by the anomalously high  $I_c$ .

438 In view of the responses of the local surface winds, relative humidity, vertical

439 motion and boundary layer to the comprehensive index of  $I_c$  mentioned above, the close  
 440 relationships between the winter mean visibility and number of hazy days over BTH  
 441 region and the given six atmospheric circulations are generally feasible in the physical  
 442 mechanism. It is reasonable and reliable to estimate the winter hazy pollutionhaze  
 443 pollutions in the BTH region based on the seasonal forecast fields derived from climate  
 444 simulation. Thus it will be helpful to provide scientific references for the governmental  
 445 decisions in advance about the reducing or controlling of pollutants emission to deal  
 446 with the probably severe hazy pollutionhaze pollutions in the BTH region.

447

448



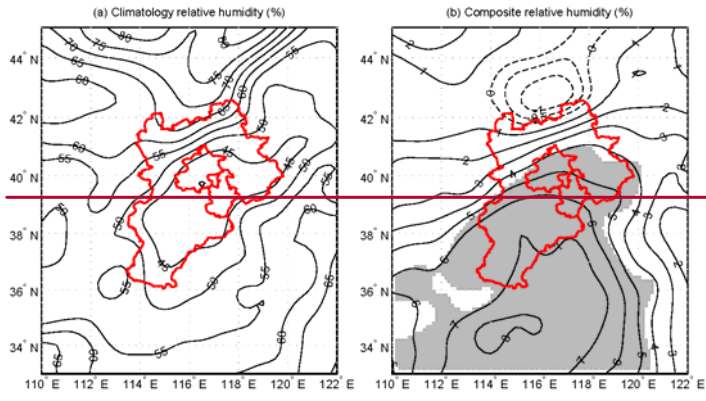
449

450 Figure 7 The climatological mean (a) and the composite (b) wind fields averaged from 1000 to 900  
 451 hPa (Area significant at the 0.05 level are shaded)  
 452

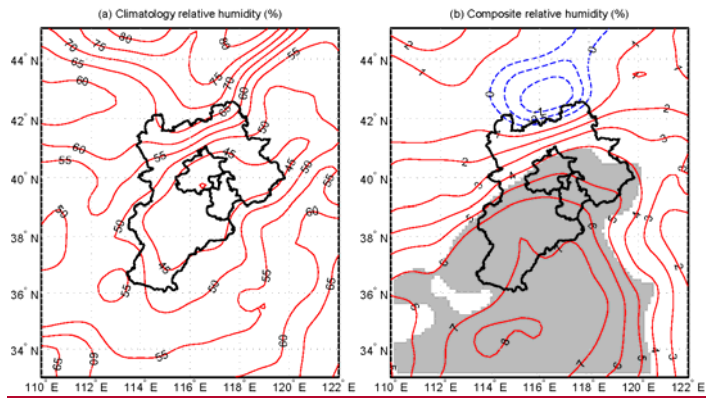
452

带格式的：居中，缩进：首行缩进： 0 字符

453



454

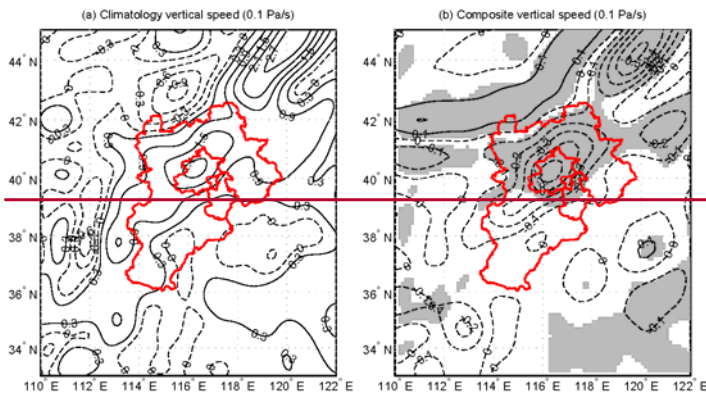


455

Figure 8 Same as Figure 7, but for relative humidity

456

457



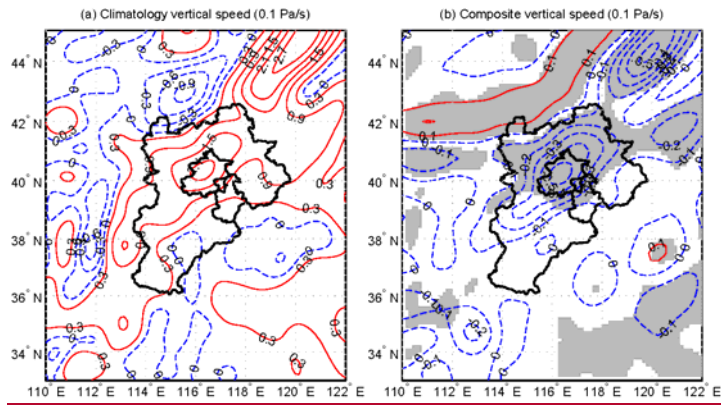


Figure 9 Same as Figure 7, but for vertical speed

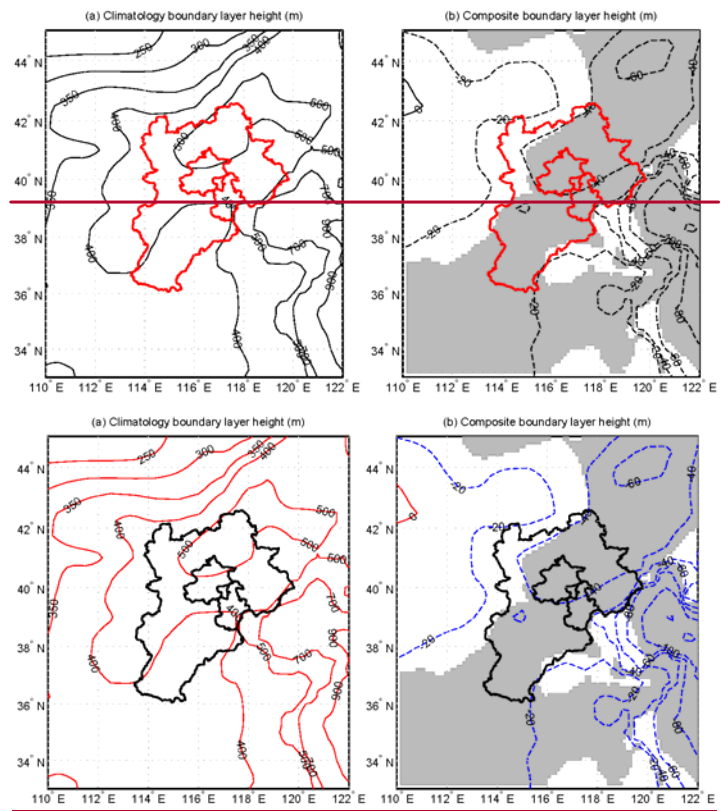


Figure 10 The climatological mean (a) and the composite (b) boundary layer height (Area significant at the 0.05 level are shaded)

465

#### 466 4 Conclusions

467 Using the daily visibility and number of hazy days recorded in the 19  
468 meteorological stations and the NCEP/NCAR and ERA-Interim reanalysis data, the  
469 evolution of the winter ~~hazy pollution~~haze pollutions in the BTH region since 1981 and  
470 their possible relations to atmospheric circulations were examined in this study.

471 The results showed that the winter mean visibility has a significantly negative  
472 correlation with the number of hazy days and both of them show distinctly inter-annual  
473 variability during the entire period 1981 to 2015. The correlation coefficients between  
474 the winter ~~hazy pollution~~haze pollutions (the visibility and number of hazy days) and  
475 the most common atmospheric circulations over the mid-high latitude of northern  
476 hemisphere were re-examined. Results showed that the relations between the ~~hazy~~  
477 ~~pollution~~haze pollutions in BTH and the winter AO, NAO and PNA were very weak,  
478 but they correlated significantly with EU, WP and SBH. Furthermore, the six new  
479 indices ( $I_1$  to  $I_6$ ) derived from the key areas in the fields of SLP, U&V850, H500, U200  
480 and T200 were closely related to the winter ~~hazy pollution~~haze pollutions in BTH. We  
481 can estimate the visibility and number of hazy days by using the six indices and the  
482 fitting and the leave-N-out cross-validation methods, respectively. In general, the high  
483 level of the estimation statistics suggested the winter ~~hazy pollution~~haze pollutions in  
484 BTH can be estimated or predicted in a reasonable degree based on the optimized  
485 atmospheric circulation indices. However, we also noted that the statistic estimation  
486 models for the visibility and number of hazy days may be influenced in part by a  
487 prominent change of the pollutants emission artificially. Thus, it is valuable and  
488 significant for government decision-making departments to take actions in advance in  
489 dealing with the probably severe ~~hazy pollution~~haze pollutions in BTH indicated by the  
490 circulation conditions, such as to control the pollutants discharge.

491 In order to investigate the link processes between the ~~hazy pollution~~haze pollutions  
492 and the given atmospheric circulations more simply, a comprehensive index ( $I_c$ ) was  
493 synthesized from the six individual circulation indices by applying a PCA method. The  
494 winter  $I_c$  increase appear to cause a shallowing of the East Asian trough at the middle  
495 troposphere and a weakening of the Siberian high pressure field at sea level, and then  
496 accompanied by a reduction (increase) of horizontal advection and vertical convection  
497 (relative humidity) in the lowest troposphere and a reduced boundary layer height in  
498 BTH and its neighboring areas, which are not conducive to the spread and elimination  
499 of air pollutants but favor the formation of ~~hazy pollution~~haze pollutions in BTH winter.



500 In short, the reasonable link processes and the stable statistic relationships suggested  
501 that the atmospheric circulation indices can be used to predict or evaluate generally the  
502 ~~hazy pollution~~haze pollutions in BTH winter to some extent.

503

#### 504 **Acknowledgments**

505 This study was supported by Beijing Natural Science Foundation (Grant no. 8152019), the National  
506 Key Technologies R & D Program of China (Grant no. 2014BAC23B01 and 2014BAC23B00) and  
507 Project ~~PE15010~~PE16010 of the Korea Polar Research Institute. X. Zhang acknowledges the  
508 financial support from the Project Z141100001014013 of Beijing Municipal Science & Technology  
509 Commission. D. Gong was supported by the National Natural Science Foundation of China (Grant  
510 No. 41321001).

#### 511 **Reference:**

- 512 An, X., Zhu, T., Wang, Z., et al.: A modeling analysis of a heavy air pollution episode  
513 occurred in Beijing, *Atmos. Chem. Phys.* 7, 3103–3114, 2007.
- 514 Baddock, M. C., Strong, C. L., Leys, J. F., Heidenreich, S. K., Tews, E. K., McTainsh,  
515 G. H.: A visibility and total suspended dust relationship, *Atmos. Environ.*, 89, 329–  
516 336, 2014.
- 517 Baumer, D., Vogel, B., Versick, S., Rinke, R., Mohler, O., Schnaiter, M.: Relationship  
518 of visibility, aerosol optical thickness and aerosol size distribution in an ageing air  
519 mass over South-West Germany, *Atmos. Environ.*, 42, 989–998, 2008.
- 520 Chan, C. K., Yao, X.: Air pollution in mega cities in China, *Atmos. Environ.*, 42, 1–42,  
521 2008.
- 522 Chang, D., Song, Y., Liu, B.: Visibility trends in six megacities in China 1973–2007,  
523 *Atmos. Res.*, 94, 161–167, 2009.
- 524 Chen, Y., Zhao, C. S., Zhang, Q., Deng, Z. Z., Huang, M. Y., Ma, X. C.: Aircraft study  
525 of mountain chimney effect of Beijing, China. *J. Geophys. Res.* 114 (D8), D08306.  
526 doi:10.1029/2008JD010610, 2009.
- 527 Dee, D. P., Uppala, S. M., Simmons, A. J., Berrisford, P., Poli, P., Kobayashi, S.,  
528 Andrae, U., Balmaseda, M. A., Balsamo, G., Bauer, P., Bechtold, P., Beljaars, A. C.  
529 M., Berg, L., Bidlot, J., Bormann, N., Delsol, C., Dragani, R., Fuentes, M., Geer, A.  
530 J., Haimberger, L., Healy, S. B., Hersbach, H., Hólm, E. V., Isaksen, L., Kållberg, P.,  
531 Köhler, M., Matricardi, M., McNally, A. P., Monge-Sanz, B. M., Morcrette, J. J.,  
532 Park, B. K., Peubey, C., Rosnay, P., Tavolato, C., Thépaut, J. N., Vitart, F.: The ERA-  
533 Interim reanalysis: Configuration and performance of the data assimilation system,  
534 *Q. J. R. Meteorol. Soc.*, 137, 553–597, 2011.

535 Deng, J. J., Xing, Z. Y., Zhuang, B. L., Du, K.: Comparative study on long-term  
536 visibility trend and its affecting factors on both sides of the Taiwan Strait, *Atmos.*  
537 *Res.*, 143, 266–278, 2014.

538 Ding, Y. H.: A statistical study of winter monsoons in East Asia, *J. Trop. Meteor.*, 6(2),  
539 119–128, 1990 (in Chinese).

540 Feng, J. L., Hu, M., Chan, C. K., Lau, P. S., Fang, M., He, L. Y., Tang, X. Y.: A  
541 comparative study of the organic matter in PM<sub>2.5</sub> from three Chinese megacities in  
542 three different climatic zones, *Atmos. Environ.* 40, 3983–3994, 2006.

543 Fritts, H. C.: *Tree-Rings and Climate*, Academic Press, London, 567pp, 1976.

544 Gao, Y., Liu, X., Zhao, C., et al.: Emission controls versus meteorological conditions  
545 in determining aerosol concentrations in Beijing during the 2008 Olympic Games,  
546 *Atmos. Chem. Phys.* 11, 12437–12451, 2011.

547 Gong, D. Y., Ho, C.H.: Siberian High and climate change over middle to high latitude  
548 Asia, *Theor. Appl. Climatol.*, 72, 1–9, 2002.

549 Gong, D. Y., Luterbacher, J.: Variability of the low-level cross-equatorial jet of the  
550 western Indian Ocean since 1660 as derived from coral proxies. *Geophys. Res. Lett.*,  
551 35, L01705, doi:10.29/2007GL032409, 2008.

552 Gong, D. Y., Zhu, J. H., Wang, S. H.: The influence of Siberian High on large-scale  
553 climate over continental Asia, *Plateau Meteor.*, 21(1), 8–14, 2002 (in Chinese).

554 Kalnay, E., Kanamitsu, M., Kistler, R., Collins, W., Deaven, D., Gandin, L., Iredell, M.,  
555 Saha, S., White, G., Woollen, J., Zhu, Y., Leetmaa, A., Reynolds, B., Chelliah, M.,  
556 Ebisuzaki, W., Higgins, W., Janowiak, J., Mo, K. C., Ropelewski, C., Wang, J., Jenne,  
557 R., Joseph, D.: The NCEP/NCAR 40-year reanalysis project, *Bull. Amer. Meteor.*  
558 *Soc.*, 77, 437–471, 1996.

559 Kang, H. Q., Zhu, B., Su, J. F., Wang, H. L., Zhang, Q. C., Wang, F.: Analysis of a long-  
560 lasting haze episode in Nanjing, China, *Atmos. Res.*, 120, 78–87, 2013.

561 Li, Y., Lu, R. Y., He, J. H.: Several climate factors influencing the winter temperature  
562 over China, *Chinese J. Atmos. Sci.*, 31(3), 505–514, 2007 (in Chinese).

563 Liu, S. H., Liu, Z. X., Li, J., Wang, Y. C., Ma, Y. J., Sheng, L., Liu, H.P., Liang, F. M.,  
564 Xin, G. J., Wang, J. H.: Numerical simulation for the coupling effect of local  
565 atmospheric circulations over the area of Beijing, Tianjin and Hebei Province, *Sci.*  
566 *China Ser. D-Earth*, 52 (3), 382–392, 2009.

567 Lo, J. C. F., Lau, A. K. H., Fung, J. C. H., Chen, F.: Investigation of enhanced cross-  
568 city transport and trapping of air pollutants by coastal and urban land-sea breeze  
569 circulations. *J. Geophys. Res.* 111 (D14), D14104. doi: 10.1029/2005JD006837,

570 2006.

571 Miao, Y. C., Liu, S. H., Zheng, Y. J., Wang, S., Chen, B. C., Zheng, H., Zhao, J. C.:

572 Numerical study of the effects of local atmospheric circulations on a pollution event

573 over Beijing–Tianjin–Hebei, China, *J. Environ. Sci.*, 30, 9–20, 2015.

574 Sabetghadam, S., Farhang, A. G., Golestani, Y.: Visibility trends in Tehran during

575 1958–2008, *Atmos. Environ.* 62, 512–520, 2012.

576 Schichtel, B. A., Husar, R. B., Falke, S. R., Wilson, W. E.: Haze trends over the United

577 States 1980–1995, *Atmos. Environ.*, 35(30), 5205–5210, 2001.

578 Streets, D. G., Fu, J. H. S., Jang, C. J., Hao, J., He, K. B., Tang, X. Y., Zhang, Y. H.,

579 Wang, Z. F., Li, Z. P., Zhang, Q., Wang, L. T., Wang, B. Y., Yu, C.: Air quality

580 during the 2008 Beijing Olympic Games, *Atmos. Environ.*, 41(3), 480–492, 2007.

581 Thompson, D. W., Wallace, J. M.: The arctic oscillation signatures in the wintertime

582 geopotential height and temperature fields, *Geophys. Res. Lett.*, 25(9), 1297–1300,

583 1998.

584 Wallace, J. M., Gutzler, D. S.: Teleconnections in the geopotential height field during

585 the Northern Hemisphere winter, *Mon. Wea. Rev.*, 109, 784–812, 1981.

586 Wang, H. J., Chen, H. P., Liu, J. P.: Arctic Sea Ice Decline Intensified Haze Pollution

587 in Eastern China, *Atmos. Oceanic Sci. Lett.*, 8(1), 1–9, 2015.

588 Wang, T., Nie, W., Gao, J., Xue, L. K., Gao, X. M., Wang, X. F., Qiu, J., Poon, C. N.,

589 Meinardi, S., Blake, D., Wang, S. L., Ding, A. J., Chai, F. H., Zhang, Q. Z., and

590 Wang, W. X.: Air quality during the 2008 Beijing Olympics: secondary pollutants

591 and regional impact, *Atmos. Chem. Phys.*, 10, 7603–7615, 2010.

592 Wang, Y., Hao, J., McElroy, M. B., 5 Munger, J. W., Ma, H., Chen, D., and Nielsen, C.

593 P.: Ozone air quality during the 2008 Beijing Olympics: effectiveness of emission

594 restrictions, *Atmos. Chem. Phys.*, 9, 5237–5251, 2009.

595 Wang, Y. S., Yao, L., Liu, Z. R., Ji, D. S., Wang, L. L., Zhang, J. K.: Formation of haze

596 pollution in Beijing–Tianjin–Hebei region and their control strategies, *Chin. Sci. Bull.*,

597 28 (3), 353–363, 2013 (in Chinese).

598 Wen, C. C., Yeh, H. H.: Comparative influences of airborne pollutants and

599 meteorological parameters on atmospheric visibility and turbidity, *Atmos. Res.*,

600 96(4), 496–509, 2010.

601 Wu, D., Chen, H. Z., Wu, M., Liao, B. T., Wang, Y. C., Liao, X. N., Zhang, X. L.,

602 Quan, J. N., Liu, W. D., Gu, Y., Zhao, X. J., Meng, J. P., Sun, D.: Comparison of

603 three statistical methods on calculating hazy days-taking areas around the capital for

604 example, *China Environ. Sci.*, 34(3), 545–554, 2014 (in Chinese).

605 Xu, W. Z., Chen, H., Li, D. H., Zhao, F. S., Yang, Y.: A case study of aerosol

606 characteristics during a haze episode over Beijing, *Procedia. Environ. Sci.* 18, 404–  
607 411, 2013.

608 Zhang, Q. H., Zhang, J. P., Xue, H. W.: The challenge of improving visibility in Beijing,  
609 *Atmos. Chem. Phys.* 10, 7821–7827, 2010.

610 Zhang, Q., Quan, J. L., Tie, X. X., Li, X., Liu, Q, Gao, Y., Zhao, D. L.: Effects of  
611 meteorology and secondary particle formation on visibility during heavy haze events  
612 in Beijing, China, *Sci. Total Environ.*, 502, 578–584, 2015.

613 Zhang, X. L., Huang, Y. B., Zhu, W. Y., Rao, R. Z.: Aerosol characteristics during  
614 summer haze episodes from different source regions over the coast city of North  
615 China Plain, *J. Quant. Spectrosc. Radiat. Transf.* 122, 180–193, 2013.

616 Zhang, Z. Y., Gong, D. Y., He, X. Z., Lei, Y. N., and Feng, S. H.: Statistical reconstruction of  
617 Antarctic Oscillation index based on multi-proxies, *Atmos. Oceanic Sci. Lett.*, 3(5),  
618 283–287, 2010.

619 Zhang, Z. Y., Gong, D. Y., Hu, M., Guo, D., He., X. Z., and Lei, Y. N.: Anomalous winter  
620 temperature and precipitation events in southern China, *J. Geogra. Sci.*, 19(4), 471–  
621 488, 2009.

622 Zhang, Z. Y., Zhang, X. L., Gong, D. Y., Quan, W. J., Zhao, X. J., Ma, Z. Q., and Kim, S. J.: Evolution  
623 of surface O<sub>3</sub> and PM<sub>2.5</sub> concentrations and their relationships with meteorological  
624 conditions over the last decade in Beijing, *Atmos. Environ.*, 108, 67–75, 2015.

625 Zhao, X. J., Zhang, X. L., Xu, X. F., Xu, J., Meng, W., and Pu, W. W.: Seasonal and diurnal  
626 variations of ambient PM<sub>2.5</sub> concentration in urban and rural environments in Beijing,  
627 *Atmos. Environ.* 43, 2893–2900, 2009.

628 Zhao, X. J., Zhao, P. S., Xu, J., Meng, W., Pu, W. W., Dong, F., He, D., and Shi, Q. F.: Analysis of a  
629 winter regional haze event and its formation mechanism in the North China Plain,  
630 *Atmos. Chem. Phys.*, 13, 5685–5696, 2013.

631

632